Testing the Br-initiated mechanism of Hg^0 oxidation

Numerous chemical transport models used for simulations of Hg cycling in the atmosphere during the past two decades considered Hg^0 reaction with ozone (O_3) and hydroxyl radical (OH) as the main Hg oxidation pathways in the free troposphere and demonstrated good agreement of modelling results with observations [e.g. *Christensen et al.,* 2004*; Pan et al.*, 2010; *Baker et al.*, 2012; *Kos et al.,* 2013; *Gencarelli et al.*, 2014; *De Simone et al.,* 2015; *Cohen et al.*, 2016]. This chemical mechanism is also included to the current EMEP operational model for Hg (GLEMOS) [*Travnikov*, 2005; *Travnikov and Ilyin*, 2009; *Travnikov et al.*, 2009]. However, more recent theoretical and observational studies show that Hg0 reactions with gaseous halogens, in particular atomic bromine (Br), should be important or even dominant pathway of Hg oxidation in the atmosphere [*Donohoue et al.*, 2006; *Hynes et al.*, 2009; *Goodsite et al.*, 2012; *Gratz et al.*, 2015; Coburn et al., 2016]. Besides, use of a simplified version of the Br oxidation mechanism in a chemical transport models allowed reproduction of realistic Hg levels in the atmosphere [*Holmes et al.*, 2010; *Soerensen et al.*, 2010; *Amos et al.*, 2012]. However, since then a number of recent studies have provided some new insight into the Hg oxidation chemistry involving Br [*Dibble et al.*, 2012; 2013, 2014; *Wang et al.*, 2014; *Jiao and Dibble*, 2015; 2017].

We evaluate possibility of implementation of the Br-initiated chemistry for the operational Hg modelling within EMEP. As a first step we incorporated the Br oxidation mechanism in its most recent form [*Horowitz et al.*, 2017] into the GLEMOS model and performed a number of tests comparing the modelling results with observations. An experimental version the model considers five Hg chemical species in the atmosphere: Hg^0 and four Hg^{II} species ($HgBr_2$, HgBrOH, $HgBrHO_2$, $HgBrNO_2$). The oxidised species Hg^{II} are simulated both in gaseous and particulate forms using the parameterisation of gas-particle partitioning from [*Amos et al.*, 2012]. A two-step mechanism of Hg^0 oxidation by atomic Br in gas phase is the following [*Horowitz et al.*, 2017]:

$$Hg^0 + X + M \rightarrow Hg^{I}X + M \qquad \text{(R1)}$$

$$Hg^{I}X + M \rightarrow Hg^0 + X + M \qquad \text{(R2)}$$

$$Hg^{I}X + Y \rightarrow Hg^0 + XY \qquad \text{(R3)}$$

$$Hg^{I}X + Y + M \rightarrow Hg^{II}XY + M \qquad \text{(R4 – R7)}$$

where X ≡ Br is the first-step Hg^0 oxidant; Y ≡ Br, OH, HO_2, NO_2 are the second-step reactants leading to reduction or further oxidation of Hg^I; and M is a molecule of air. The reaction rate constants are given in Table 1. Six-hourly concentration fields of Br were archived from a GEOS-Chem simulation [*Parrella et al.,* 2012], whereas OH, HO_2, NO_2 and particulate matter (PM2.5) fields were imported from MOZART [*Emmons et al.*, 2010]. We performed simulations for the period 2007-2013 using anthropogenic emissions for 2010 [*AMAP/UNEP*, 2013]. The first 6 years of the period were used for the model spin

up to achieve the steady-state Hg concentrations in the troposphere. The model results are presented as annual averages for 2013.

Table 1. *Experimental chemical mechanism for atmospheric Hg in GLEMOS*

N	Reaction	Rate, molecule cm^{-3} s^{-1}	Reference
R1	$Hg^0 + Br + M \rightarrow HgBr + M$	$1.5 \times 10^{-32} (T/298)^{-1.86} [Hg^0][Br][M]$ (a)	*Donohoue et al.,* 2006
R2	$HgBr + M \rightarrow Hg^0 + Br + M$	$1.6 \times 10^{-9} \exp(-7801/T) [HgBr][M]$	*Dibble et al.,* 2012
R3	$HgBr + Br \rightarrow Hg^0 + Br_2$	$3.9 \times 10^{-11} [HgBr][Br]$	*Balabanov et al.,* 2005
R4	$HgBr + Br \xrightarrow{M} HgBr_2$	$2.5 \times 10^{-10} (T/298)^{-0.57} [HgBr][Br]$	*Goodsite et al.,* 2004
R5	$HgBr + OH \xrightarrow{M} HgBrOH$	$2.5 \times 10^{-10} (T/298)^{-0.57} [HgBr][OH]$	*Goodsite et al.*, 2004
R6	$HgBr + HO_2 \xrightarrow{M} HgBrHO_2$	$k_{HO2}([M],T)[HgBr][HO_2]$	*Jiao and Dibble,* 2017
R7	$HgBr + NO_2 \xrightarrow{M} HgBrNO_2$	$k_{NO2}([M],T)[HgBr][NO_2]$	*Jiao and Dibble,* 2017

Figure 1 shows simulated global distributions of Hg^0 surface concentration and Hg wet deposition as well as their comparison with observations. A collection of data on Hg^0 air concentrations and Hg wet deposition fluxes measured at various regional and global monitoring networks in 2013 involved in the study are described in [*Travnikov et al.*, 2017]. Generally, the spatial patterns are similar to those obtained with the O_3/OH chemical mechanism [*Travnikov et al.*, 2009]. The concentration pattern demonstrates the well documented south-to-north increasing gradient and elevated concentrations in East and South Asia (Fig. 1a). The wet deposition pattern also shows relatively high levels over the industrial regions, in areas with intensive precipitation and over the Southern ocean, where intensive Hg oxidation takes place (Fig. 1b). It should be pointed out that the modelling results significantly underestimate measured Hg^0 concentrations, particularly, in remote regions of the Southern Hemisphere, where the effect of the atmospheric chemistry is the most pronounced. This is not the case for simulated wet deposition fluxes, which are comparable with the observed ones. The reasons for this contradiction are discussed below.

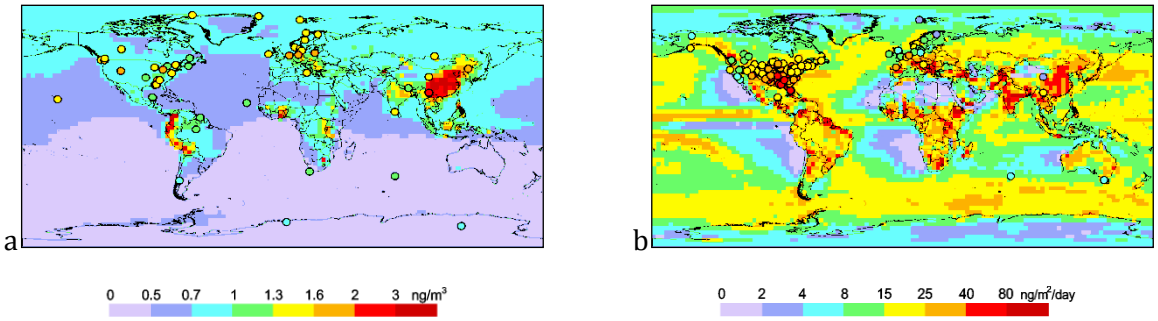

Fig. 1. *Spatial distributions of simulated* Hg^0 *surface concentration (a) and* Hg *wet deposition (b) in 2013. Circles show observed values in the same colour scale.*

More detailed evaluation of the modelling results against observations is illustrated in Fig. 2. As seen the model underestimates the observed values by 40% on average (Fig. 2a). The underprediction is stronger for low concentrations typical for remote regions. A

few elevated values are relatively well reproduced by the model. These values relate to sites located in East Asia, which are characterised by direct effect of anthropogenic emissions. In contrast, the simulated wet deposition does not underestimate or in some cases even overestimates the measurements (Fig.2a). This imbalance between too low simulated Hg^0 concentration and high wet deposition can be explained by too strong *in situ* oxidation of Hg^0 and production of Hg^{II} in the atmosphere. Indeed, if biased low Hg^0 air concentration can be additionally explained by uncertainties in emissions of this species (anthropogenic, natural or secondary), Hg wet deposition is largely formed by scavenging of Hg^{II}, which is mostly originated from Hg^0 oxidation in remote regions. So hypothetical increase of Hg emissions would shift both measured characteristics upward leading to overestimation of wet deposition. Thus, the analysis shows that the current mechanism of Hg0 oxidation by atomic Br taken alone leads to too strong Hg oxidation in the atmosphere, which does not agree with available measurements.

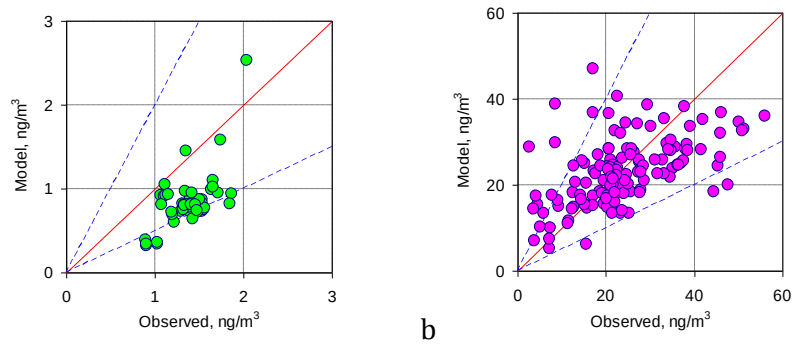

a b

Fig. 2. *Comparison of simulated* Hg^0 *air concentration (a) and* Hg *wet deposition (b) with measurements in 2013.*

Some more insight to the oxidation process can be obtained from analysis of the Hg chemical budget in the atmosphere (Fig. 3). The simulated global atmospheric reservoir of Hg^0 is about 1600 Mg that is significantly lower than previously estimated 4000 Mg for the total atmosphere [e.g. *Travnikov et al.*, 2009; *Holmes et al.*, 2010] or 3500 Mg for the troposphere [*Horowitz et al.*, 2017].The gas-phase oxidation by atomic Br leads to transformation of 4850 Mg/y of Hg^0 to a short-lived intermediate HgBr. It corresponds to the chemical lifetime 3.9 months of Hg^0 against oxidation to HgBr. The unstable HgBr decomposes back to Hg^0 or reacts further with various atmospheric compounds (e.g. Br, OH, HO_2, NO_2) to form Hg^{II}. Decomposition of HgBr reduces 870 Mg/year of Hg^I to the elemental form. The simulated Hg^{II} species are dominated by $HgBrNO_2$, which contributes 67% of total atmospheric oxidized Hg. The second largest Hg^{II} species is $HgBrHO_2$ (20%), which is followed by $HgBr_2$ (8%) and HgBrOH (4%).

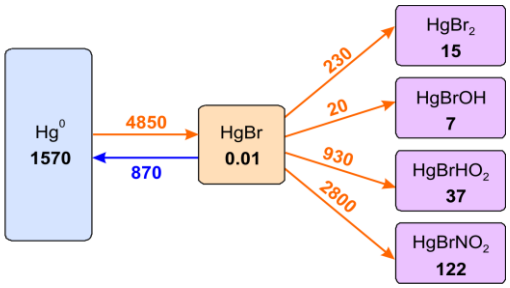

Fig. 3. *Global budget of* Hg *chemical cycling in the atmosphere. The mass estimates are in* Mg *of Hg, the fluxes are in* Mg *of* Hg *per year.*

Appropriate production rates vary from 20 Mg/y for HgBrOH to 2800 Mg/y for $HgBrNO_2$. So the net oxidation of Hg^0 to Hg^{II} depends on both the first-step Hg^0 reaction with Br and on the balance between decomposition and further oxidation of the HgBr intermediate.

Figure 4 shows the simulated latitudinal and vertical distribution of annual zonal mean Hg^0 air concentration (standard temperature and pressure) in the atmosphere. As seen the surface concentration of Hg^0 is above 0.7 ng/m^3 in the Northern Hemisphere and drops steeply south of the equator. In the vertical, the concentration moderately decreases in the troposphere down to 0.1 ng/m^3 at the tropopause. The latitudinal pattern of Hg^0 concentration is determined by both distribution of emissions, which are mostly located in the Northern Hemisphere, and the oxidation chemistry. The figure also shows distribution of the annual mean Hg^0 oxidation rate (isolines) in reaction with Br (R1, Table 1). The rate depends on concentration of Br as well as on the ambient parameters such as air temperature and density. The Hg^0 oxidation has a minimum in the free troposphere over the equator due to elevated air temperatures, and two maximums – in the upper troposphere and over in the surface air of the temperate latitudes of the Southern Hemisphere – due to high concentration of Br. These extremes are reflected in the spatial pattern of Hg^0 by increased concentrations over the equator and low concentrations over the Southern Ocean.

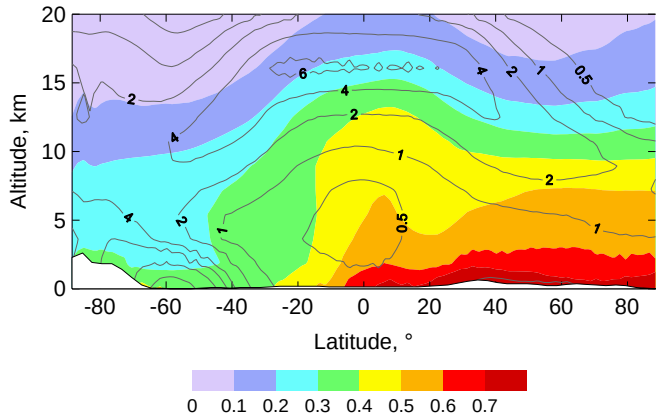

Fig. 4. *Annual zonal mean air concentration of* Hg^0 *in 2013 (colour palette, ng/m³ STP) and rates of* Hg^0 *oxidation by* Br *(isolines,* 10^6 s^{-1}*) according to reaction R1 from Table 1.*

Formation of the Hg^{II} species is illustrated in Fig. 5. The figure shows distribution of average mixing ratios of $HgBr_2$, HgBrOH, $HgBrHO_2$, and $HgBrNO_2$ in the atmosphere along with production rates of these species in appropriate reactions (R4-R7, Table 1). The reaction rates depend on production of HgBr, concentration of appropriate oxidants (Br, OH, HO_2, NO_2), and air temperature. The dominant Hg^{II} species $HgBrNO_2$ is largely produced in the upper troposphere and next to the surface in the high latitudes of the Southern Hemisphere (Fig. 5d). However, intensive dry and wet deposition quickly removes this species from the surface air. In contrast, Hg^{II} produced in the upper

troposphere has longer residence time that leads to its accumulation and high concentrations aloft. The second important Hg^{II} species is $HgBrHO_2$ is intensively produced at high latitudes of the Northern and, in particular, Southern Hemispheres (Fig. 5c). These regions are also characterized by relatively high concentrations of the species in the free troposphere. Both $HgBr_2$ and HgBrOH have maximums of production rates in the upper troposphere of the tropics and near the surface at high latitudes of the Southern Hemisphere, where elevated concentrations of these species occur (Fig. 5a and b). There are also increased concentrations over the surface at temperate latitudes of the Northern Hemisphere, which are caused by direct anthropogenic emissions. All Hg^{II} species have small concentrations in the low troposphere of the tropics due to reduced production of HgBr in this area and high air temperature, which is damping its further oxidation to Hg^{II}.

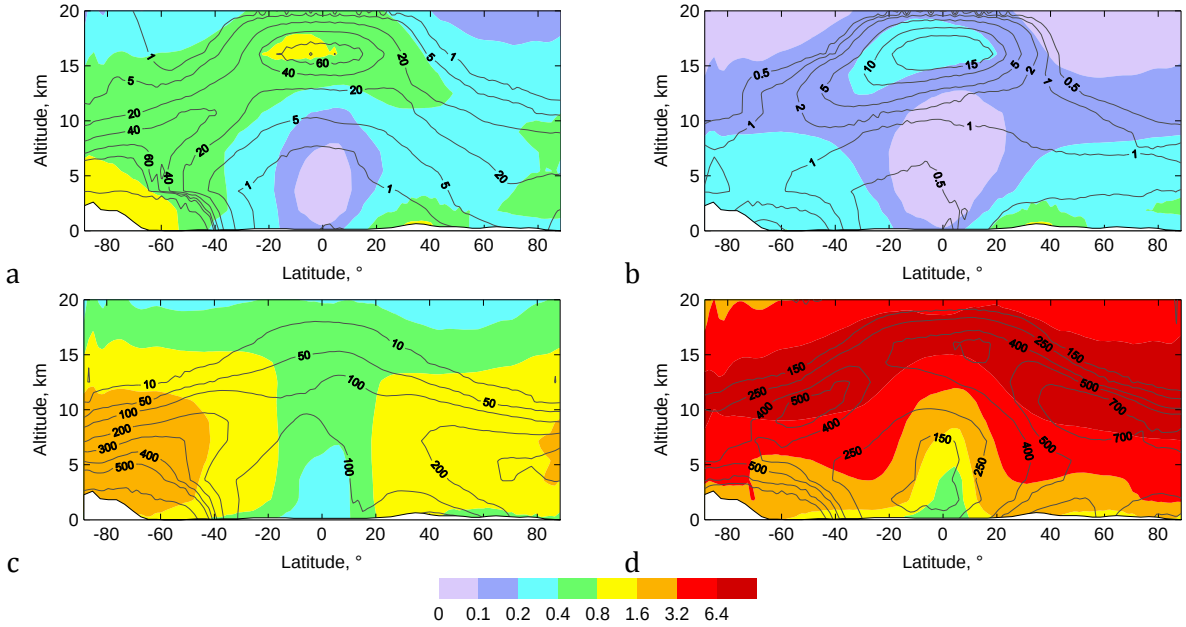

Fig. 5. *Annual zonal mean volume mixing ratios (colour palette,* ppqv Hg*) of* $HgBr_2$ *(a),* HgBrOH *(b),* $HgBrHO_2$ *(c),* $HgBrNO_2$ *(d) in 2013. Isolines show production rates (*10^3 *molecules* cm^{-3} s^{-1}*) for appropriate Hg species according to reactions R4-R7 from Table 1.*

Thus, use of the Br-initiated mechanism for simulations of Hg atmospheric cycle leads to strong overestimation of Hg oxidation and unrealistically low Hg^0 concentrations in the atmosphere. However, theoretical studies point out at possibility of Hg^{II} reduction mechanisms, which could take place in air, cloud water, or heterogeneously at the surface of atmospheric aerosol [*Ariya et al.,* 2015]. Besides, a number of modelling studies have successfully applied the Br oxidation mechanism along with a hypothetical reduction mechanism to reproduce observed concentrations [*Shah et al.,* 2016; *Horowitz et al.,* 2017]. But it should be noted that both nature and chemical details of the reduction reaction remain unknown.

AMAP/UNEP [2013] Technical Background Report for the Global Mercury Assessment 2013a. Arctic Monitoring and Assessment Programme, Oslo, Norway / UNEP Chemicals Branch, Geneva, Switzerland, vi + 263 pp., available at: http://www.amap.no/documents/download/1265 (last access: 10 April 2018).

Amos H.M., Jacob D.J., Holmes C.D., Fisher J.A., Wang Q., Yantosca R.M., Corbitt E.S., Galarneau E., Rutter A.P., Gustin M.S., Steffen A., Schauer J.J., Graydon J.A., Louis V.L. St., Talbot R.W., Edgerton E.S., Zhang Y., and Sunderland E.M. [2012] Gas-particle partitioning of atmospheric Hg(II) and its effect on global mercury deposition, *Atmos. Chem. Phys.*, **12**, 591–603, doi:10.5194/acp-12-591-2012.

Ariya P.A., Amyot M., Dastoor A., Deeds D., Feinberg A., Kos G., Poulain A., Ryjkov A., Semeniuk K., Subir M. & Toyota K. [2015] Mercury Physicochemical and Biogeochemical Transformation in the Atmosphere and at Atmospheric Interfaces: A Review and Future Directions, *Chemical Reviews* **115**(10), 3760-3802.

Baker K.R. and Bash J.O. [2012] Regional Scale Photochemical Model Evaluation of Total Mercury Wet Deposition and Speciated Ambient Mercury, *Atmos. Environ.*, **49**, 151–162.

Balabanov N., Shepler B., Peterson K. [2005] Accurate global potential energy surface and reaction dynamics for the ground state of HgBr2*, J. Phys. Chem.* A, **109**, 8765—8773.

Christensen J.H., Brandt J., Frohn L.M. and Skov H. [2004] Modelling of Mercury in the Arctic with the Danish Eulerian Hemispheric Model, *Atmos. Chem. Phys.*, **4**, 2251–2257, doi:10.5194/acp-4-2251-2004.

Coburn S., B. Dix, E. Edgerton, C. D Holmes, D. Kinnison, Q. Liang, A. Ter Schure, S. Wang, and R. Volkamer (2016) Mercury oxidation from bromine chemistry in the free troposphere over the southeastern US, *Atmospheric Chemistry and Physics*, **16**(6), 3743–3760, doi:10.5194/acp-16-3743-2016.

Cohen M.D., Draxler R.R., Artz R.S., Gustin M., Han Y.-J., Holsen T.M., Jaffe D., Kelley P., Lei H., Loughner C., Luke W., Lyman S., Niemi D. Pacyna J.M., Pilote M., Poissant L., Ratte D., Ren X., Steenhouisen F., Tordon R. and Wilson S. [2016] Modeling the global atmospheric transport and deposition of mercury to the Great Lakes, Elementa: *Science of the Anthropocene*, 4, 000118, doi:10.12952journal.elementa.999118.

De Simone F., Cinnirella S., Gencarelli C.N., Yang X., Hedgecock I.M., and Pirrone N. [2015] Model study of global mercury deposition from biomass burning, *Environ. Sci. Technol.*, **49**, 6712–6721.

Dibble T.S., M.J. Zelie and H. Mao [2012] Thermodynamics of reactions of ClHg and BrHg radicals with atmospherically abundant free radicals. *Atmospheric Chemistry and Physics*, 12:10271-10279.

Dibble T.S., M.J. Zelie and H. Mao [2013] Corrigendum to "Thermodynamics of reactions of ClHg and BrHg radicals with atmospherically abundant free radicals" published in *Atmospheric Chemistry and Physics*, **12**:10271-10279, 2012. *Atmospheric Chemistry and Physics*, **13**:9211-9212.

Dibble T.S., M.J. Zelie and Y. Jiao [2014] Quantum chemistry guide to PTRMS studies of as yet undetected products of the bromine atom initiated oxidation of gaseous elemental mercury. *Journal of Physical Chemistry* A, **118**:7847-7854.

Donohoue D., Bauer D., Cossairt B., and Hynes A. [2006] Temperature and pressure dependent rate coefficients for the reaction of Hg with Br and the reaction of Br with Br: A pulsed laser photolysispulsed laser induced fluorescence study, *J. Phys. Chem.* A, **110**, 6623–6632, doi:10.1021/jp054688j.

Emmons L.K., Walters S., Hess P.G., Lamarque J.-F., Pfister G.G., Fillmore D., Granier C., Guenther A., Kinnison D., Laepple T., Orlando J., Tie X., Tyndall G., Wiedinmyer C., Baughcum S.L., and Kloster S. [2010] Description and evaluation of the Model for Ozone and Related chemical Tracers, version 4 (MOZART-4), *Geosci. Model Dev.*, **3**, 43–67, doi:10.5194/gmd-3-43-2010.

Gencarelli C.N., De Simone F., Hedgecock I.M., Sprovieri F., and Pirrone N. [2014] Development and Application of a Regional-Scale Atmospheric Mercury Model Based on WRF/Chem: A Mediterranean Area Investigation. *Environ. Sci. Pollut.* R., **21**, 4095–4109.

Goodsite M.E., Plane J.M.C. and Skov H. [2004] A Theoretical Study of the Oxidation of Hg0 to HgBr2 in the Troposphere, *Environ. Sci. Technol.*, **38**, 1772–1776.

Goodsite M.E., Plane J.M.C. and Skov H. [2012] Correction to A Theoretical Study of the Oxidation of Hg^0 to HgBr2 in the Troposphere, *Environ. Sci. Technol.*, **46**, 5262, doi:10.1021/es301201c.

Gratz L.E., Ambrose J.L., Jaffe D.A., Shah V., Jaegle L., Stutz J., Festa J., Spolaor M., Tsai C., Selin N.E., Song S., Zhou X., Weinheimer A.J., Knapp D.J., Montzka D.D., Flocke F.M., Campos T.L., Apel E., Hornbrook R., Blake N.J., Hall S., Tyndall G.S., Reeves M., Stechman D., and Stell M. [2015] Oxidation of mercury by bromine in the subtropical Pacific free troposphere, *Geophysical Research Letters*, **42**, 10.1002/2015gl066645.

Holmes C.D., Jacob D.J., Corbitt E.S., Mao J., Yang X., Talbot R., and Slemr F. [2010] Global atmospheric model for mercury including oxidation by bromine atoms, *Atmos. Chem. Phys.*, **10**, 12037–12057, doi:10.5194/acp-10-12037-2010.

Horowitz H.M., D.J. Jacob, Y. Zhang, T.S. Dibble, F. Slemr, H.M. Amos, J.A. Schmidt, E.S. Corbitt, E.A. Marais and E.M. Sunderland [2017] A new mechanism for atmospheric mercury redox chemistry: Implications for the global mercury budget. *Atmospheric Chemistry and Physics Discussions*, **1-33**, 10.5194/acp-2016-1165.

Hynes A.J., Donohoue D.L., Goodsite M.E., and Hedgecock I.M. [2009] Our Current Understanding of Major Chemical and Physical Processes Affecting Mercury Dynamics in the Atmosphere and At the Air-Water/Terrestrial Interfaces, in: Mercury Fate and Transport in the Global Atmosphere, edited by: Pirrone N., and Mason R., Springer Science Business Media, LLC, 427–457.

Jiao Y. and Dibble T.S. [2017] First kinetic study of the atmospherically important reactions BrHg + NO2 and BrHg + HOO, *Phys. Chem. Chem. Phys.*, **19**, 1826–1838, doi:10.1039/c6cp06276h.

Jiao Y. and T.S. Dibble [2015] Quality structures, vibrational frequencies, and thermochemistry of the products of reaction of BrHg• with NO2, HO2, ClO, BrO, and IO. *Journal of Physical Chemistry* A, 119:10502-10510.

Kos G., Ryzhkov A., Dastoor A., Narayan J., Steffen A., Ariya P.A., and Zhang L. [(2013] Evaluation of discrepancy between measured and modelled oxidized mercury species, *Atmos. Chem. Phys.*, **13**, 4839–4863, doi:10.5194/acp-13-4839-.

Pan L., Lin C.-J., Carmichael G.R., Streets D.G., Tang Y., Woo J.-H., Shetty S.K., Chu H.-W., Ho T.C., and Friedli H.R. [2010] Study of Atmospheric Mercury Budget in East Asia Using STEM-Hg Modeling System, *Sci. Total Environ.*, **408**, 3277–3291.

Parrella J.P., Jacob D.J., Liang Q., Zhang Y., Mickley L. J., Miller B., Evans M.J., Yang X., Pyle J.A., Theys N., and Van Roozendael M. [2012] Tropospheric bromine chemistry: implications for present and pre-industrial ozone and mercury, *Atmos. Chem. Phys.*, **12**, 6723–6740, doi:10.5194/acp-12-6723-2012.

Shah V., Jaeglé L., Gratz L.E., Ambrose J.L., Jaffe D.A., Selin N.E., Song S., Campos T.L., Flocke F.M., Reeves M., Stechman D., Stell M., Festa J., Stutz J., Weinheimer A.J., Knapp D.J., Montzka D.D., Tyndall G.S., Apel E.C., Hornbrook R.S., Hills A.J., Riemer D.D., Blake N.J., Cantrell C.A., and Mauldin III R.L. [2016] Origin of oxidized mercury in the summertime free troposphere over the southeastern US, *Atmos. Chem. Phys.,* **16**, 1511–1530, doi:10.5194/acp-16-1511-2016.

Soerensen A.L., Sunderland E.M., Holmes C.D., Jacob D.J., Yantosca R.M., Skov H., Christensen J.H., Strode S.A., and Mason R.P. [2010] An improved global model for air-sea exchange of mercury: high concentrations over the north Atlantic, *Environ. Sci. Technol.*, **44**, 8574–8580.

Travnikov O., Angot H., Artaxo P., Bencardino M., Bieser J., D'Amore F., Dastoor A., De Simone F., Diéguez M. D. C., Dommergue A., Ebinghaus R., Feng X. B., Gencarelli C. N., Hedgecock I. M., Magand O., Martin L., Matthias V., Mashyanov N., Pirrone N., Ramachandran R., Read K. A., Ryjkov A., Selin N. E., Sena F., Song S., Sprovieri F., Wip D., Wängberg I., and Yang X. [2017] Multi-model study of mercury dispersion in the atmosphere: atmospheric processes and model evaluation, *Atmos. Chem. Phys.*, **17**, 5271-5295, doi:10.5194/acp-17-5271-2017.

Travnikov O. and Ilyin I. [2009] The EMEP/MSC-E Mercury Modeling System, in: Mercury Fate and Transport in the Global Atmosphere: Emissions, Measurements, and Models, edited by: Pirrone, N. and Mason, R. P., *Springer*, 571–587.

Travnikov O., Jonson J.E., Andersen A.S., Gauss M., Gusev A., Rozovskaya O., Simpson D., Sokovyh V., Valiyaveetil S., and Wind P. [2009] Development of the EMEP global modelling framework: Progress report. EMEP/MSC-E Technical Report 7/2009, Meteorological Synthesizing Centre – East of EMEP, Moscow, 44 pp., available at: http://www.msceast.org/index.php/publications/reports (last access: 19 June 2018).

Travnikov O. [2005] Contribution of the intercontinental atmospheric transport to mercury pollution in the Northern Hemisphere. *Atmos. Environ.*, **39**, 7541–7548.

Wang F. Saiz-Lopez A., Mahajan A.S., Gómez Martín J.C., Armstrong D., Lemes M., Hay T., and Prados-Roman C. [2014] Enhanced production of oxidised mercury over the tropical Pacific Ocean: A key missing oxidation pathway. *Atmos. Chem. Phys.* **14**, 1323–1335.